Aminofunctionalization Effect on the Microtribological Behavior of Carbon Nanotube/Bismaleimide Nanocomposites

Lina Liu,[1] Zhengping Fang,[1,2] Aijuan Gu,[3] Zhenghong Guo[2]

[1]*Institute of Polymer Composites, Zhejiang University/Key Laboratory of Macromolecular Synthesis and Functionalization, Ministry of Education, Hangzhou 310027, People's Republic of China*
[2]*Lab of Polymer Materials and Engineering, Ningbo Institute of Technology, Zhejiang University, Ningbo 315100, People's Republic of China*
[3]*Materials Engineering Institute, Soochow University, Suzhou, Jiangsu 215021, People's Republic of China*

Received 24 April 2008; accepted 29 January 2009
DOI 10.1002/app.30156
Published online 8 May 2009 in Wiley InterScience (www.interscience.wiley.com).

ABSTRACT: Original multiwalled carbon nanotubes (O-MWCNTs) and aminofunctionalized ethylenediamine-treated multiwalled carbon nanotubes (MWCNTs-EDA) were mixed with bismaleimide (BMI) resin to prepare O-MWCNT/BMI and MWCNT-EDA/BMI composites, respectively. Raman spectroscopy, thermogravimetric analysis, and infrared spectroscopy were used to investigate the influence of aminofunctionalization on the multiwalled carbon nanotube (MWCNT) framework. Dynamic mechanical analysis, scanning electron microscopy images of the fractured surface, and field emission scanning electron microscopy of the worn surface were used to determine the possible friction and wear mechanisms of the system. The MWCNT-EDA/BMI composite exhibited a higher friction coefficient value and a lower wear loss rate value than the O-MWCNT/BMI composite, which was attributed to the larger number of defects caused by the aminofunctionalization of the MWCNTs, the stronger interfacial adhesion formed between the MWCNTs-EDA and the BMI resin, and the better dispersive state of the MWCNTs-EDA in the BMI matrix. © 2009 Wiley Periodicals, Inc. J Appl Polym Sci 113: 3484–3491, 2009

Key words: composites; interfaces; polyimides

INTRODUCTION

Carbon nanotubes (CNTs) have demonstrated a remarkably high potential for mechanical and physical properties because of their structure, size, and topology[1–4]; this has made them attractive for various applications, especially as nanotube-reinforced materials in nanocomposites, nanoelectronic devices, and so on.[5] Since the first report of the low-friction properties of CNTs,[6] researchers have begun to investigate the tribological behaviors of CNT composites, including CNT/copper,[7] CNT/Ni-P,[8,9] CNT/carbon,[10] CNT/polyimide,[11] CNT/polytetrafluroethylene,[12] CNT/poly(methyl methacrylate),[13] and CNT/epoxy nanocomposites.[14] It was reported that the composites reinforced by CNTs displayed improved friction and wear properties compared with the pure substrate matrix because of the special effects of CNTs.[15,16]

However, most of research work has focused on the external influence on CNT-reinforced composites, such as the temperature and hardness of the composites, and the effect of the inner factors, such as the interfacial strength of the composite, have been neglected, which is a key problem for CNT-reinforced composite systems. Also, there have been almost no investigations into the effect of CNTs' alteration and modification of the tribological properties of the composites, which may pave an important path to the study of the wear mechanisms of the composites. According to the problems mentioned previously, aminofunctionalized CNTs were chosen in this study for further investigation.

Before our study, it was also of great importance to choose a suitable kind of resin as our matrix, whose physical, mechanical, and tribological properties would affect the final properties of the composites. Bismaleimides (BMIs) are quite attractive to the advanced composite industry for their excellent properties in hot and wet environment and their great potential to be used as wear-resistant materials.[17–21] Many modified BMI resin systems have been developed to meet the requirements for various applications. Among them, a two-component, high-performance resin system based on 4,4′-bismaleimidodiphenylmethane (BDM) and *o,o*′-diallylbisphenol A (DBA), coded as BDM/DBA, has proven to have outstanding toughness, good humidity resistance, and

Correspondence to: Z. Fang (zpfang@zju.edu.cn).
Contract grant sponsor: Natural Science Foundation; contract grant number: 50473037.

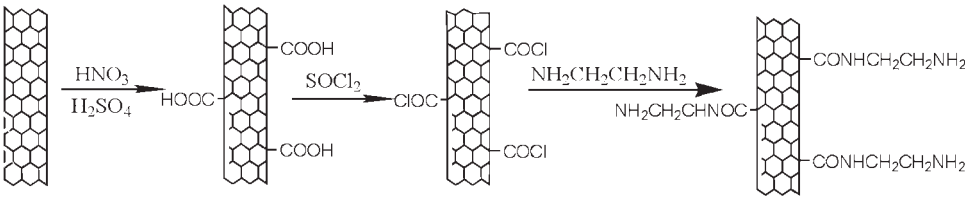

Figure 1 Preparation process of the MWCNTs-EDA from O-MWCNTs.

excellent thermal and mechanical properties.[22] In addition, the hydroxyl group of the resin can react with the amino group on the surface of multiwalled carbon nanotubes (MWCNTs). So, this BDM/DBA resin system was chosen as the matrix in this study.

The goal of this study was to examine the influence of the surface characteristics of CNTs on the tribological behavior of composites through the incorporation of aminofunctionalized CNTs into the BMI resin and to determine the main mechanism that took effect during the process.

EXPERIMENTAL

Materials

BDM was supplied by HuBei Fengwang Chemicals (Hubei, China), and DBA was provided by Northwestern Polytechnical University (Xi'an, China).

The MWCNTs were obtained from Chengdu Organic Chemicals Co., Ltd. (Chengdu, China). The properties of the CNTs were as follows: purity $>$ 95%, average diameter = 20–30 nm, average length $<$ 50 μm. They were prepared by a catalytic chemical vapor deposition method.

Amination of the MWCNTs

The brief preparation process of the ethylenediamine-treated multiwalled carbon nanotubes (MWCNTs-EDA) is shown in Figure 1. The MWCNTs were purified and shortened with a mixture of nitric and sulfuric acid (1:3 by volume), and in this step, the carboxyl groups were imported onto the surface of the MWCNTs. The shortened MWCNTs (ca. 1 mg) in 200 mL of $SOCl_2$, together with 10 mL of dimethylformamide, were stirred at 20°C for 24 h. After purification, the mixture of the chlorocarbonylized MWCNTs and ethylenediamine (EDA) was refluxed at 120°C for 96 h. After the mixture was cooled to room temperature, the excess EDA was removed by washing with ethanol several times. The remaining solid was filtered through a membrane with a pore diameter of 0.22 μm. The collected solid was washed with ethanol several times. Then, the resulting black solid was dried at room temperature *in vacuo* before the measurements. Here, we designate the untreated original MWCNTs and EDA-treated MWCNTs as O-MWCNTs and MWCNTs-EDA, respectively.

Preparation of the MWCNT/BMI nanocomposites

MWCNTs (0.1 g) were added to DBA (4.4 g) at room temperature with vigorous agitation. The mixture was stirred mechanically for 2 h; this was followed by ultrasonic agitation for another 2 h to get a homogeneous suspension. Then, the suspension was added to 5.5 g of BDM at 130°C with stirring for 15 min. The resulting mixture was poured into a preheated mold and degassed in a vacuum oven at 130°C for 1 h. Finally, the mixture was cured in a vacuum oven according to the following conditions: 140°C for 2 h, 160°C for 2 h, 180°C for 2 h, and 200°C for 2 h. The mixture was postcured in an air atmosphere at 220°C for 12 h. So, a 1 wt % MWCNT/BMI composite was prepared, and to prepare a 1 wt % MWCNT-DBA/BMI composite, 0.95 g of BDM was added to the system to adjust to the uniform network as the former system. Composites with different MWCNT and MWCNT-DBA contents were prepared with a similar process to that mentioned previously.

Characterization

Fourier transform infrared spectroscopy (FTIR)

FTIR spectra of the O-MWCNTs and MWCNTs-EDA were taken at an ambient temperature of 25°C with a Bruker Vector 22 FTIR spectrometer with the KBr pellet method.

Raman spectroscopy

Raman spectra were obtained with a Thermo Nicolet Ahmega Dispersive Raman spectrometer with an Nd:YAG laser and a liquid N_2 cooled Ge detector with laser excitation at 672 nm.

Thermogravimetric analysis (TGA)

This test was performed with a Universal V3.8B instrument in the temperature range 80–850°C at a heating rate of 15°C/min under flowing nitrogen.

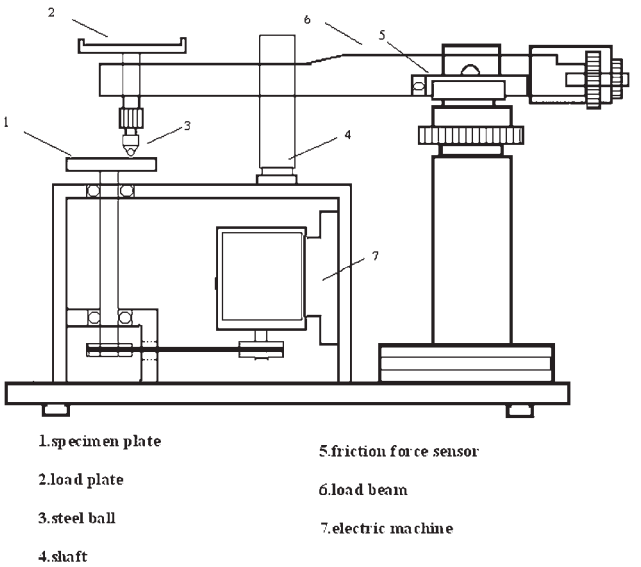

Figure 2 Schematic diagram of the wear and friction testing machine.

Field emission scanning electron microscopy (FESEM)

The surface morphology of the samples and the dispersive state of the MWCNTs in BMI resin were observed with a field emission scanning electron microscope (Sirion, FEI). Before observation, the surface of the samples was sprayed with a thin, even film of gold to improve the conductivity of the surface.

Dynamic mechanical analysis

This test was performed under tensile mode with a DMA242C dynamic mechanical analyzer (Netzsch Co., Germany). All runs were performed with a frequency of 1 Hz and a heating rate of 5°C/min.

Friction and wear tests

The friction and wear tests were conducted on a WTM-E atmosphere changeable model friction and wear tester (Lanzhou Physical and Chemistry Institute, Lanzhou, China). The schematic diagram of the friction and wear tests is shown in Figure 2. A plain steel ball with a diameter of 3 mm was used as the counterpart material. Sliding was performed under air conditions with an ambient temperature of around 25°C over a period of 1 h at a sliding velocity of 0.84 m/s and a normal load of 50 N. Before testing, all specimens were cleaned; that is, the specimens were abraded with water-abrasive paper (no. 240), superfine water-abrasive paper, and a liquid diamond polishing agent successively. Then, both the steel ball and the specimens were cleaned with acetone and distilled water and dried at 70°C. The friction force was measured with a torque shaft equipped with strain gauges, and we calculated the friction coefficient automatically by taking into account the normal load and the friction force measured. Mass loss was measured with an especially accurate analytical balance at an interval of 30 min throughout the tests. Taking repeatability into account, we obtained the test results from the friction and wear tests of steady-state sliding under dry conditions from three readings, and the average value was used in our results.

RESULTS AND DISCUSSION

Characterization of the MWCNTs-EDA

As shown in Figure 3, the Raman spectra for the O-MWCNTs and MWCNTs-EDA beyond the Raman D and G bands (D-band is assigned to the disordered graphite structure or sp_3-hybridized carbons of the nanotubes, and G-band corresponds to a splitting of the E_{2g} stretching mode of graphite), the second-order modes (2D and $2E_{2g}$), the second-order combination (D + E_{2g}), and frequencies were detected readily in the both O-MWCNTs and MWCNT-EDA samples. The defect-induced dispersive D band was positioned around 1342 cm^{-1}, the graphite-related mode G band was positioned at 1583 cm^{-1}, and the highly dispersive second harmonic Raman phonon peak D-band overtone (2D band) was positioned from 2670 to 2680 cm^{-1}. The additional bands around 2918 and 3224 cm^{-1} corresponded to the E_{2g} + D and $2E_{2g}$ combination frequencies, respectively.[23] It was obvious that the intensities of the D, G, and 2D peak values (designated as I(D), I(G) and I(2D) respectively) showed a sharp increase in the MWCNT-EDA sample, which meant that more defects and sp^3-hybridized carbons were formed on the MWCNT surface. The increase in sp^3-hybridized carbons in the MWCNT framework showed that the

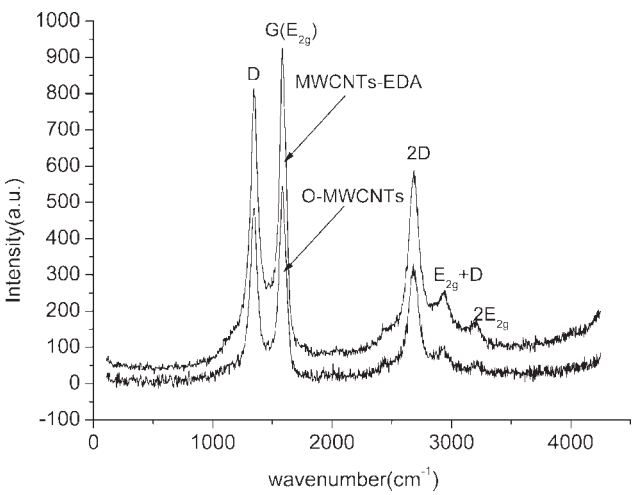

Figure 3 Raman spectra for the O-MWCNTs and MWCNTs-EDA.

TABLE I
Raman Features for the O-MWCNTs and MWCNTs-EDA

Sample	Peak (cm^{-1})	Intensity (au)	I(G)/I(D)	I(G)/I(2D)
O-MWCNTs	(D) 1342.78	484.0634	1.121	0.551
	(2D) 2677.23	299		
	(G) 1583.84	542.6155		
MWCNTs-EDA	(D) 1344.71	802.5068	1.152	0.635
	(2D) 2683.07	587.1711		
	(G) 1581.91	924.3525		

MWCNT structure was changed and a covalent attachment to the MWCNTs was generated. Here, we used I(G)/I(D) and I(G)/I(2D) to evaluate the efficient covalent functionalization of the MWCNTs; the detailed data are shown in Table I. As shown in Table I, I(G)/I(D) and I(G)/I(2D) for the MWCNT-EDA sample showed larger values than they did in the O-MWCNT sample, which indicated that some functional groups were attached onto the MWCNT framework. The derivative thermogravimetry (DTG) peak around 250°C of the MWCNT-EDA sample indicated the attachment of functional groups to the MWCNTs, too. The exact chemical structure of the functional groups that were attached to the MWCNT surfaces was characterized by an FTIR spectrum (Fig. 4). Compared with the O-MWCNTs, the spectrum of the MWCNTs-EDA showed peaks at 3455 cm^{-1} [the overlap of the ν(O—H) stretch modes of O—H and ν(—N—H—) and the stretch modes of N—H in the chain of the carbonyl group], 2955 cm^{-1} [the ν(—CH_2—) stretch modes of —CH_2— in the chain of —CH_2—NH_2], 1631 cm^{-1} [the δ(C=O) bending modes of C=O of the carbonyl group], 1537 cm^{-1} [the ν(N—H) stretch modes of N—H in the end chain of the NH_2 group], 1507 cm^{-1} [the δ(N—H) bending modes of N—H in the chain of the NH_2 group], and 1480 cm^{-1} [the ν(—CH—CO—) stretch modes of the —CH—CO— chain].

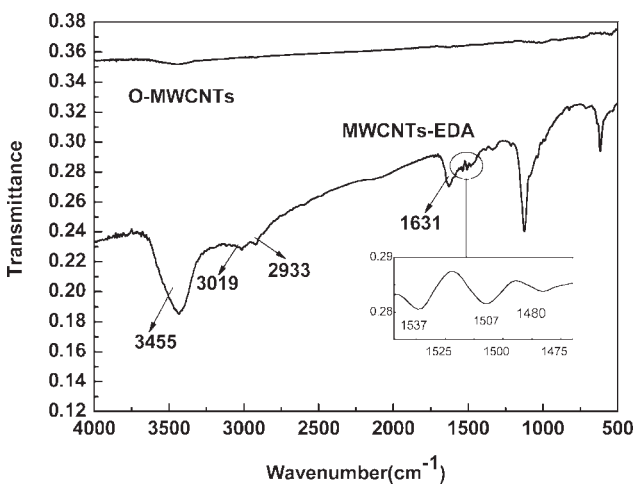

Figure 4 FTIR spectra for the O-MWCNTs and MWCNTs-EDA.

Friction and wear behavior for the O-MWCNT/BMI composites

Generally, the friction coefficient and wear loss rate are the most commonly used parameters for characterizing the tribological properties of materials, although different testing machines may be used to obtain these two important parameters. Figure 5 gives the friction coefficient of the O-MWCNT/BMI composite as a function of MWCNT content. Obviously, the incorporation of MWCNTs into the BMI matrix decreased the friction coefficient and wear rate values and caused better wear-resistance properties than those in the pure BMI resin. With the addition of MWCNTs, the friction coefficient displayed a decreasing trend. Figure 6 shows the wear loss rate of the O-MWCNT/BMI composite as a function of MWCNT content. The wear loss rate decreased considerably with increasing MWCNT content before the MWCNT content value arrived at 2.5 wt %. When the MWCNT content value surpassed 2.5 wt %, the wear loss rate of the composite showed a slight increase with increasing amount of MWCNTs.

This phenomenon was attributed to the excellent self-lubrication properties of MWCNTs because they are composed of concentric cylindrical layers or

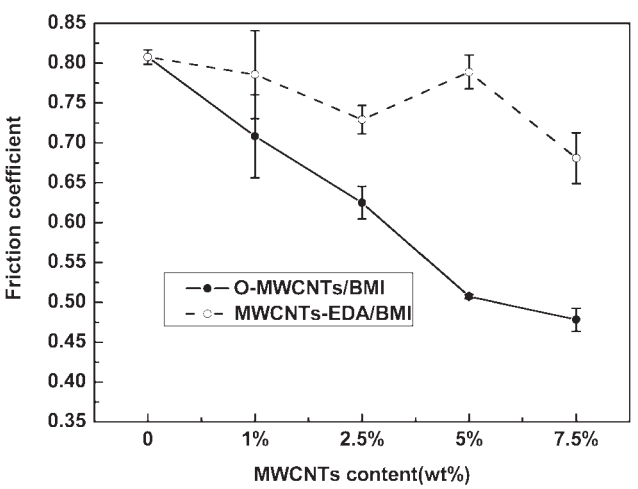

Figure 5 Variation of the friction coefficient with the content of MWCNTs for the O-MWCNT/BMI and MWCNT-EDA/BMI composites.

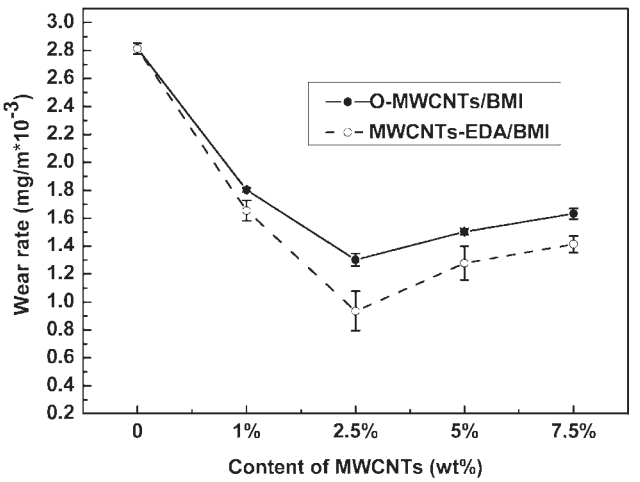

Figure 6 Variation of the wear loss rate with the content of MWCNTs for the O-MWCNT/BMI and MWCNT-EDA/BMI composites.

shells of graphitelike sp^2-bonded cylindrical layers or shells. The intershell interaction is predominately controlled by the van der Waals forces, so MWCNTs can easily slide or rotate with each other; this leads to good self-lubricating properties.[24–26] For composites with MWCNTs as nanofillers, MWCNTs in the matrix near the surface are exposed and act as the lubricating thin film on the worn surface, which will produce a smoother worn surface (discussed later in the article) and improved wear resistance compared to the pure BMI resin without MWCNT reinforcement. Furthermore, this self-lubricating effect was strengthened with the increasing addition of MWCNTs into the BMI resin. The improvement in the friction and wear behavior for the O-MWCNT/BMI composite up to a content of 2.5 wt % demonstrate this conclusion. Similar results were also reported by other researchers.[27,28]

Friction and wear properties of the MWCNT-EDA/BMI composites

From Figure 5, it is obvious that the friction coefficient decreased from 0.808 for the pure BMI resin to 0.478 for 7.5 wt % addition of O-MWCNTs, whereas the friction coefficient of the MWCNT/BMI composite decreased to 0.68. This indicated that the addition of the MWCNTs helped to decrease the friction coefficient of the composite but not so much as the addition of the O-MWCNTs. Also, the addition of the MWCNTs-EDA helped to decrease the friction coefficient of the composite but not so much as the addition of the O-MWCNTs. This was because the aminofunctionalization caused physical damage to the outer surface of the MWCNTs and broke some carbon bonds in the prism planes. Also, all of these changes affected the lubricating effect of the MWCNTs. The increased intensity value of the defect-indicating D band for the MWCNTs-EDA in the Raman spectra (shown in Fig. 3 and Table I) gave detailed information about this damage. Figure 7 shows that MWCNT-EDA weight loss was as high as 31.73% (which showed the weight loss for EDA decomposition around 250°C), whereas that of the O-MWCNTs was only 11.53% at 850°C. This decreased thermostability of the MWCNTs-EDA compared with the O-MWCNTs also illustrated this damage to the MWCNTs. The comparison of the FESEM images between the O-MWCNTs and MWCNTs-EDA gave a more direct illustration of this damage. Compared with O-MWCNTs shown in Figure 8(a), the rougher surface and more caps in the MWCNT-EDA sample, as shown in Figure 8(b), distinctly indicated the damage caused by the aminofunctionalization of the MWCNTs. Also, the damage to the MWCNT framework reduced their self-lubricating effect. In addition, the attachment of EDA to MWCNT surface changed sp^2 bonds to sp^3 bonds and added to the interaction force of cylindrical layers or shells, so the interrotation was hindered to some degree, and the self-lubricating effect of the MWCNTs was thus weakened. On the other hand, the diameter of the MWCNTs was enlarged a little after aminofunctionalization. This diameter enlargement of the MWCNTs also decreased the friction behavior of the MWCNT-reinforced composites.

Figure 6 gives the wear loss rate of both the O-MWCNT/BMI composite and MWCNT-EDA/BMI composite as a function of MWCNT content. The addition of the MWCNTs-EDA into the BMI resin also decreased the wear loss rate of the material from 2.813×10^{-3} to 1.301×10^{-3} mg/m at 2.5 wt %. Moreover, the MWCNT-EDA/BMI composite displayed a lower wear loss rate value over the whole MWCNT content variation range than the O-MWCNT/BMI composite. This phenomenon was

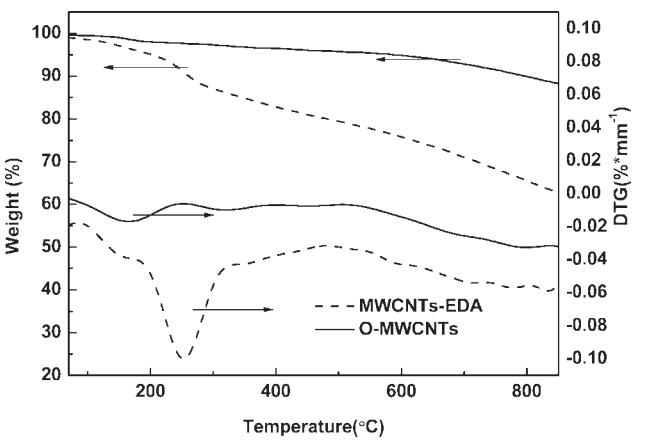

Figure 7 TGA and DTG curves for the O-MWCNTs and MWCNTs-EDA.

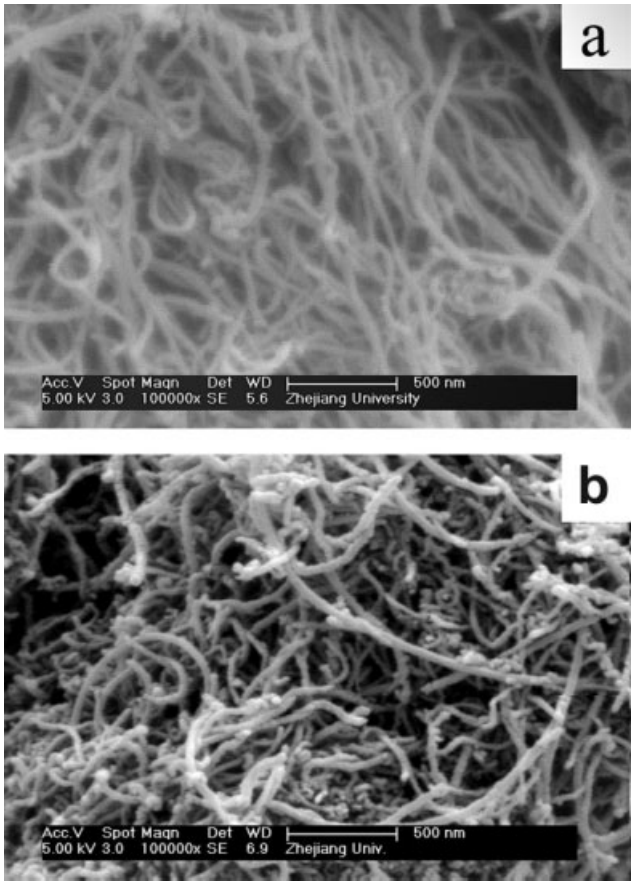

Figure 8 FESEM images of the (a) O-MWCNTs and (b) MWCNTs-EDA.

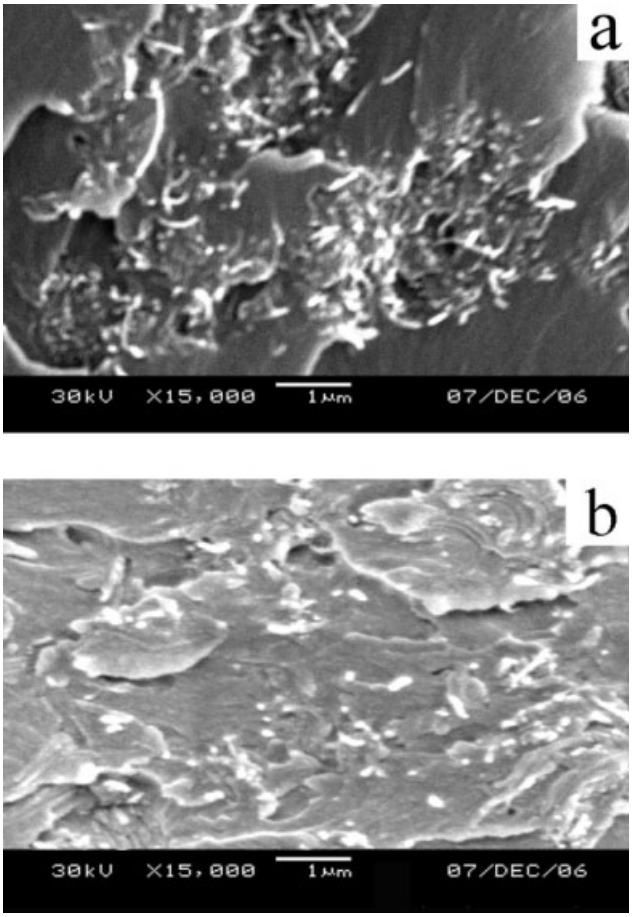

Figure 9 SEM pictures of the fracture surfaces of the MWCNT1/BMI composites: with 2.5 wt % (a) O-MWCNTs and (b) MWCNTs-EDA.

related to the better dispersion situation of the MWCNTs-EDA in the BMI matrix and the improved interface between the MWCNTs-EDA and the BMI matrix. As shown in the SEM pictures for the fracture surface of the MWCNT/BMI composites in Figure 9, it is clear that the MWCNTs-EDA dispersed more evenly in the BMI resin and had less agglomeration than the O-MWCNT/BMI composite. According to the self-lubricating effect of the MWCNTs mentioned previously, the MWCNTs in the matrix near the surface acted as a lubricating thin film on the worn surface. Then, the good dispersion conditions of the MWCNTs-EDA in the BMI matrix meant that the component of the lubricating thin film was uniform, and obviously, a uniform film is good for improving the wear resistance of a composite. This can also be interpreted as the reason why there was a threshold of the concentration of MWCNTs in the matrix (Fig. 6) for the wear loss rate of the composites; when the concentration of MWCNTs in the matrix was bigger than the threshold (2.5 wt %), the wear loss rate of the composites did not continuously decrease with increasing concentration of MWCNTs in the matrix because a higher concentration of MWCNTs in the matrix tended to lead to a poorer dispersion of MWCNTs in the BMI matrix.

On the other hand, the better interfacial adhesion between the MWCNTs-EDA and the BMI matrix

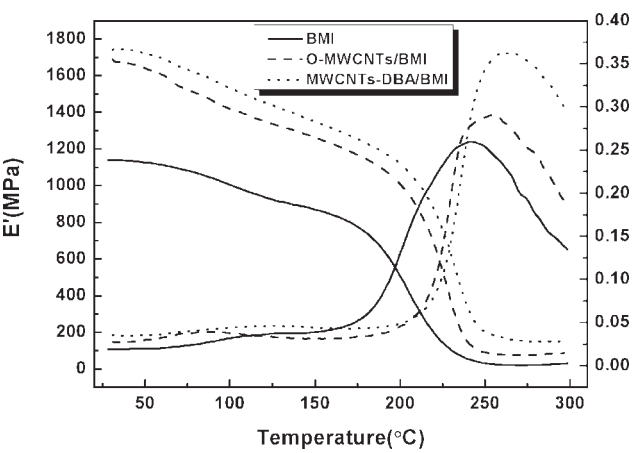

Figure 10 Storage modulus (E') and loss tangent (tan δ) values of the pure BMI resin, O-MWCNT/BMI composite, and MWCNT-EDA/BMI composite as a function of temperature with a MWCNT content of 2.5 wt %.

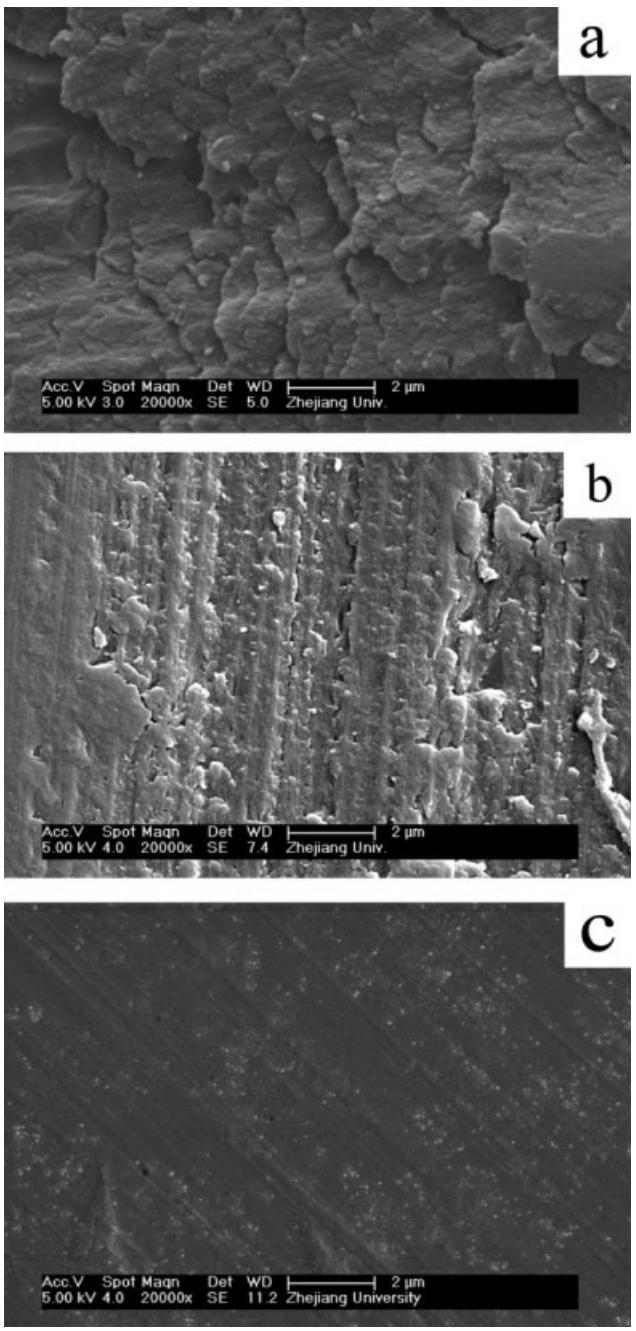

Figure 11 FESEM images of the worn surfaces of the (a) pure BMI resin, (b) O-MWCNT/BMI composite, and (c) MWCNT-EDA/BMI composite with a MWCNT content of 2.5 wt % under dry sliding friction conditions.

was an important factor in obtaining good wear resistance. Excellent interfacial adhesion between the MWCNTs and the matrix meant that, during the tribological process, the MWCNTs were more difficult to peel out from the matrix and increased the lubricating effect of the carbon film. In our system, the amino group of the MWCNTs-EDA reacted with the hydroxyl group of the prepolymer of the BMI resin; this resulted in a denser and more stable network of MWCNTs-EDA/BMI. The improvement of the vitrification point (T_g) of MWCNT-EDA/BMI shown in Figure 10 indicated that a denser and more stable network was formed compared with the O-MWCNT/BMI composite.[29,30] The firmer network indicated a stronger interfacial adhesion in the MWCNT-EDA/BMI composite than in O-MWCNT/BMI and, thus, better wear-resistant properties.

Wear mechanism of the MWCNT/BMI composite

To further confirm the explanation of the effect of the aminofunctionalization of the MWCNTs on the wear behavior of the MWCNT/BMI composites, the morphologies of the worn surfaces were obtained by FESEM. As shown in Figure 11(a), the worn surface of the pure BMI resin was rough, and many scratching grooves, petal-like cracks, and debris were found there, which showed that the pure BMI resin had relatively poor wear resistance in its sliding against the steel counterpart and its tribological mechanism may have followed an adhesive wear mechanism. After the addition of O-MWCNTs to the BMI resin, the worn surface of the composite became smoother, and a large number of petal-like flanges on the BMI surface turned into slots [see Fig. 11(b)]. In the case of the MWCNT-EDA/BMI composite, a uniform and smooth surface was found, as shown in Figure 11(c), with fewer cracks and scales. The even and tiny grooves cut by the granules from the block sample showed that the MWCNT-EDA/BMI composite displayed the typical pattern of the microabrasive friction mechanism.[31–33] All these images of the wear surface were in good conformity with the improved wear resistance of the MWCNT-EDA/BMI composite and our interpretation for it.

CONCLUSIONS

The MWCNT-EDA reinforced BMI composite was used here to investigate the influence of surface modification on the friction and wear properties of the composites. The differences in the friction and wear properties between the O-MWCNT/BMI and MWCNT-EDA/BMI composites were attributed to the self-lubricating property of the MWCNTs, interfacial adhesion between the MWCNTs and BMI, and the MWCNTs dispersive state in the BMI matrix. Specifically speaking, aminofunctionalization triggered defects in the MWCNTs, which thus reduced the self-lubricating effects of the MWCNTs and increased the friction coefficients of the MWCNT-EDA/BMI composite. On the other hand, the aminofunctionalization of the MWCNTs strengthened the interface between the MWCNTs and the BMI resin and enhanced the dispersive state of the MWCNTs in the BMI matrix, which led to a more even and uniform worn surface and decreased the wear loss

rate. Moreover, the dispersive state of the MWCNTs also played an important role in the presence of the threshold concentration value of the MWCNTs at 2.5 wt %. The main wear mechanism of the composite changed from adhesive mode to typical abrasive mode because of the aminofunctionalization of the MWCNTs, in good accordance with the results we have summarized.

References

1. Wong, E. W.; Sheehan, P. E.; Lieber, C. M. Science 1997, 277, 1971.
2. Falvo, M. R.; Clary, G. J.; Taylor, R. M.; Chi, V.; Brooks, F. P.; Washburn, S.; Superfine, R.Nature 1997, 389, 582.
3. Krishnan, A.; Dujardin, E.; Treacy, M. M. J.; Hugdahl, J.; Lynum, S.; Ebbesen, T. W. Nature 1997, 388, 451.
4. Baughman, R. H.; Zakhidov, A. A.; de Heer, W. A. Science 2002, 297, 787.
5. Friend, R. H.; Gymer, R. W.; Holmes, A. B.; Burroughes, J. H.; Marks, R. N.; Taliani, C.; Bradley, D. D. C.; Dos Santos, D. A.; Bredas, J. L.; Logdlund, M.; Salaneck, W. R. Nature 1999, 397, 121.
6. Cumings, J.; Zettl, A.Science 2000, 289, 602.
7. Tu, J. P.; Yang, Y. Z.; Wang, L. Y.; Ma, X. C.; Zhang, X. B. Tribology Lett 2001, 10, 225.
8. Chen, W. X.; Tu, J. P.; Wang, L. Y.; Gan, H. Y.; Xu, Z. D.; Zhang, X. B. Carbon 2003, 41, 215.
9. Lim, D. S.; An, J. W.; Lee, H. J. Wear 2002, 252, 512.
10. Yang, Z.; Xu, H.; Li, M. K.; Shi, Y. L.; Huang, Y.; Li, H. L. Thin Solid Films 2004, 466, 86.
11. Cai, H.; Yan, F. Y.; Xue, Q. J. Mater Sci Eng A 2004, 364, 94.
12. Chen, W. X.; Li, F.; Han, G.; Xia, J. B.; Wang, L. Y.; Tu, J. P.; Xu, Z. D. Tribology Lett 2003, 15, 275.
13. Yang, Z.; Dong, B.; Huang, Y.; Liu, L.; Yan, F. Y.; Li, H. L. Mater Lett 2005, 59, 2128.
14. Sulong, A. B.; Park, J.; Lee, N.; Goak, J. J Compos Mater 2006, 40, 1947.
15. Zoo, Y. S.; An, J. W.; Lim, D. P.; Lim, D. S. Tribology Lett 2004, 16, 305.
16. An, J. W.; You, D. H.; Lim, D. S. Wear 2003, 255, 677.
17. Liang, G. Z.; Gu, A. J. Bismaleimides; Chemical Industry Press: Beijing, 1997.
18. Ramulu, M.; Young, P.; Kao, H.J Mater Eng Perform 1999, 8, 330.
19. Pilato, L. A.; Michno, M. J. Advanced Composite Materials; Springer-Verlag: Berlin Heidelberg, 1994.
20. Milano, J. C.; Mekkid, S.; Vernet, J. L. Eur Polym J 1998, 34, 717.
21. Liang, G. Z.; Fan, J.J Appl Polym Sci 1999, 73, 1623.
22. Chaudhari, M.; Galvin, T; King, J.SAMPE J 1985, 21, 17.
23. Okpalugo, T. I. T.; Papakonstantinou, P.; Murphy, H.; Mclaughlin, J.; Brown, N. M. D. Carbon 2005, 43, 2951.
24. Iijima, S.Nature 1991, 354, 56.
25. Kolmogorov, A. N.; Crespi, V. H. Phys Rev Lett 2000, 85, 4727.
26. Crespi, V. H.; Zhang, P.; Lammert, P. E. Electronic Properties of Novel Materials Science and Technology of Molecular Nanostructures; American Institute of Physics: New York, 1999.
27. Chen, X. H.; Chen, C. S.; Xiao, H. N.; Liu, H. B.; Zhou, L. P.; Li, S. L.; Zhang, G.Tribology Int 2006, 39, 22.
28. Wang, L. Y.; Tu, J. P.; Chen, W. X.; Wang, Y. C.; Liu, X. K.; Olk, C.; Cheng, D. H.; Zhang, X. B. Wear 2003, 254, 1289.
29. Xue, Q.; Zhang, L. N. Modern Research Methods in Polymer Physics; Wuhan University Press: Wuhan, China, 2002.
30. Allen, G.; Bevington, J. C. Comprehensive Polymer Science: The Synthesis, Characterization, Reaction and Application of Polymers; Pergamon Press Inc.: New York, 1989.
31. Li, M. H.; Zhuang, Z. Tribology; Xi'an Jiaotong University Press: Xi'an, China, 1988.
32. Ge, S. R. Introduction to Tribology; China Machine Press: Beijing, 2007.
33. Peter, A. A. Impact Wear of Materials; IBM System Production Division: New York, 1976.